Catena 254 (2025) 108947

Contents lists available at ScienceDirect

Catena

journal homepage: www.elsevier.com/locate/catena

Carbon dynamics in termite mounds: The effect of land use on microbial oxalotrophy

Teneille Nel [a], Catherine E. Clarke [a,*], Michele L. Francis [a], Darya Babenko [b], Alf Botha [b], Daniel O. Breecker [c], Don A Cowan [d], Timothy Gallagher [e], Pedro Lebre [d], Joseph R. McAuliffe [f], Alyssa N. Reinhardt [e], Marla Trindade [g]

[a] Department of Soil Science, Stellenbosch University, Victoria Street, Stellenbosch 7600, South Africa
[b] Department of Microbiology, Stellenbosch University, Victoria Street, Stellenbosch 7600, South Africa
[c] Department of Earth and Planetary Science, the University of Texas at Austin, Austin, TX, USA
[d] Centre for Microbial Ecology and Genomics, Department of Biochemistry, Genetics and Microbiology, University of Pretoria, Pretoria 0002, South Africa
[e] Department of Earth Science, Kent State University, Kent, OH, USA
[f] Department of Research, Conservation & Collections, Desert Botanical Garden, Phoenix, AZ, USA
[g] Institute for Microbial Biotechnology and Metagenomics, Department of Biotechnology, University of the Western Cape, Bellville 7535, South Africa

ARTICLE INFO

Keywords:
Functional biodiversity
Oxalate-carbonate pathway
Semi-arid regions
Soil inorganic carbon
Termite mounds

ABSTRACT

The semi-arid western region of South Africa hosts extensive earthen mounds known as *heuweltjies*, which are inhabited by *Microhodotermes viator* termites and play a critical role in soil biogeochemical cycling. These mounds accumulate significant stores of soil organic and inorganic carbon (C), including pedogenic calcium carbonate, which may form through microbially induced calcite precipitation. In this study, the effects of land use change on C dynamics in *heuweltjie* soils were assessed by examining soil biogeochemistry and apparent respiratory quotient (ARQ, based on soil pore gas composition). We investigated the oxalate-carbonate pathway (OCP) as a potential mechanism of C sequestration. Topsoils were collected from one pristine and one cultivated termite mound in a semi-arid region of South Africa and incubated for one week. The carbon dioxide (CO_2) and oxygen concentrations of soil pore gas as well as chemical properties of soils treated with termite frass (excrement) or calcium oxalate (CaOx) were monitored. Increases in pH and the calcite saturation index in both CaOx- and frass-treated soils suggested the potential occurrence of the OCP. The ARQ values did not reflect geochemical changes associated with OCP due to competing metabolic pathways, such as potential lignin degradation in frass-treated soils. Higher ARQ values in uncultivated versus cultivated CaOx-treated soils may indicate higher carbon use efficiency in uncultivated soils or destabilization of existing C in cultivated soils. Respiration in frass-treated soils was higher than control and CaOx-treated soils and resulted in production of bicarbonate (via dissociation of carbonic acid formed by dissolution of respired CO_2 in water). This implies that termite-affected landscapes may sequester C in inorganic form. Increased total C in both cultivated and uncultivated soils treated with frass suggests that microbial CO_2-fixation may occur in termite-affected landscapes, necessitating further investigation of pathways responsible for this process.

1. Introduction

The Greater Cape Floristic region of South Africa is home to broad, low-relief earthen mounds (known as *heuweltjies*) occupied by colonies of *Microhodotermes viator* (southern harvester termite) (McAuliffe, 2022). *Heuweltjies*, which can occupy more than a quarter of the land surface in these regions, support high biodiversity due to their unique soil physicochemical properties (Midgley et al., 2002). The harvesting of plant material by termites for processing and storage results in localized concentrations of plant-derived nutrients and salts in the mounds (Clarke et al., 2022; McAuliffe et al., 2019; Midgley et al., 2012) as well as significant stores of carbon (C) compared to the surrounding soils (Clarke et al., 2023; Francis et al., 2024). Continuous deposition of termite excrement, which is particularly abundant in the case of *M. viator*, is also an important source of C in the mounds (Swanepoel, 2021; Vermonti, 2022). The elevated C levels within these mounds may

* Corresponding author.
E-mail address: cdowding@sun.ac.za (C.E. Clarke).

https://doi.org/10.1016/j.catena.2025.108947
Received 15 October 2024; Received in revised form 7 March 2025; Accepted 14 March 2025
Available online 22 March 2025
0341-8162/© 2025 The Author(s). Published by Elsevier B.V. This is an open access article under the CC BY license (http://creativecommons.org/licenses/by/4.0/).

reflect a reduction of atmospheric carbon dioxide (CO_2) levels via sequestration and stabilization of C in soils, thereby providing a nature-based solution to combat global climate change (Seddon et al., 2020).

Carbon cycle models prioritize above-ground biomass and soil organic C (SOC) (Berthelin et al., 2022), despite carbonates in drylands comprising over a third of global C stocks in the form of soil inorganic C (SIC) (Hirt et al., 2023; Lal et al., 2021). SIC accumulation with depth (Harrison et al., 2011; Jin et al., 2014) results from carbonate precipitation via leaching or capillary Ca^{2+} movement. *Heuweltjies* often contain pedogenic calcium carbonate ($CaCO_3$) (Clarke et al., 2023; Francis et al., 2024; Midgley et al., 2012) that may have formed via microbially-induced calcite precipitation (MICP). MICP is the process of $CaCO_3$ precipitation, catalysed by enzymes produced by bacteria and fungi. Dissolved inorganic C (DIC) is produced as a result of respiration-associated CO_2 dissolution and is the essential precursor for MICP, a process which is also catalyzed by bacterial and fungal enzymes. Therefore, MICP results in transformation of microbially respired CO_2-C into mineral form (Wang et al., 2023). Pedogenic calcite can only be considered a net-sink of atmospheric CO_2 if the Ca^{2+} comes from a non-calcareous source, otherwise its formation is simply a result of dissolution and re-precipitation of parent material (Groshans et al., 2019; Laudicina et al., 2021; Monger & Martinez-Rios, 2000). Marine aerosols have been shown to be the major source of salts, including Ca, along the South African west coast (Clarke et al., 2022; Francis et al., 2024; Nyaga et al., 2013; van Gend et al., 2021). Therefore, microbially-induced conversion of organic carbon to inorganic carbon as soil carbonates, in dry climates, or as aqueous bicarbonate, in humid regions (Hartmann *et al.*, 2013; Monger et al., 2015), can be an important pathway of atmospheric carbon sequestration in termite-affected soils.

Many plant species in the Greater Cape Floristic Region, particularly shrubby leaf succulents in the family Mesembryanthemaceae, accumulate significant quantities of calcium oxalate (CaOx) in their tissues (Vermonti et al., 2025). Oxalotrophy, which is the ability of organisms to utilize oxalate as a carbon source (Kost et al., 2014), can provide a mode of MICP in CaOx-rich ecosystems (Monger et al., 2015). This occurs via the oxalate-carbonate pathway (OCP) (Palmieri et al., 2019), whereby oxalotrophic bacteria and fungi decompose (oxidize) CaOx in organic matter, release Ca^{2+} into solution and increase soil pH. This drives precipitation of calcite from the soil DIC pool (Hervé et al., 2021; Pons et al., 2018; Uren, 2018). The OCP may be a means to sequester C, as the formation of CaOx removes four moles of C from the atmosphere, while only two moles of C are released as CO_2 during calcite precipitation. The series of reactions associated with the OCP are as follows:

$$CaC_2O_4 \rightarrow Ca^{2+} + C_2O_4^{2-} \quad (1)$$

$$2C_2O_4^{2-} + O_2 + 4H^+ \rightarrow 2H_2CO_3 + 2CO_2 \quad (2)$$

$$H_2CO_3 \rightarrow H^+ + HCO_3^- \quad (3)$$

$$Ca^{2+} + 2HCO_3^- \rightarrow CaCO_3 + H_2O + CO_2 \quad (4)$$

The net reaction can be written as (Cowan et al., 2024):

$$2CaC_2O_4 + O_2 + 2H^+ + 2HCO_3^- \rightarrow 2CaCO_3 + 2\,H_2O + 4CO_2 \quad (5)$$

Oxalate species may enter the soil via microbial decomposition of plant litter or termite frass containing oxalate salts (Cowan et al., 2024; Gadd et al., 2014; Hervé et al., 2021). Once released from organic matter, CaOx is rapidly oxidized via microbially catalysed metabolic reactions (Hervé et al., 2016; Martin et al., 2012). Thus, oxalates occur in low concentrations in soils (e.g., 0.01 – 2.5 μmol CaOx g^{-1} soil in temperate forests (Certini et al., 2000; Dauer & Perakis, 2014)) despite relative insolubility and thermodynamic stability of this biomineral (Brecevic & Kralj, 2010; Uren, 2018; Verrecchia et al., 2006). Oxalate salts serve multiple biological roles in plants including provision of CO_2 via crystal decomposition during stomatal closure (Tooulakou et al., 2016). This drought-adaptation strategy may explain the greater occurrence of plant species containing CaOx crystals in areas with lower mean annual rainfall (Garvie, 2006; Karabourniotis et al., 2020). There is a growing appreciation that the global scale of the OCP is sufficiently large to be an important contribution to global carbon turnover budgets (Cowan et al., 2024).

The importance of CaOx in biochemical cycles may have been underestimated previously due to the difficulties involved in identification and quantification of chemical oxalate species in soils (Misiewicz & Vanwert, 2022). Regular, high-precision monitoring of soil pore space CO_2 and O_2 concentrations may provide a novel approach to study transformations of CaOx non-destructively, both spatially and temporally in soils. This approach is based on the concept of the Respiratory Quotient (RQ), which is the ratio of CO_2 produced relative to O_2 consumed during respiration (Dilly, 2001). Measurements of soil pore space CO_2/ O_2 values are referred to as "apparent" respiratory quotient values (ARQ) after correcting for differing diffusion rates of the two gases (Angert et al., 2015; Bergel et al., 2017; Hodges et al., 2019), which yields the equation:

$$ARQ = -0.76 * \frac{d\,CO_2}{d\,O_2} \quad (6)$$

The primary control on the RQ is the oxidation state of carbon in the substrate being respired (Dilly, 2001; Hicks Pries et al., 2020; Masiello et al., 2008) In oxalate compounds, the oxidation state of C is equal to + 3, which results in a much higher RQ (4) for oxidation of oxalate compared to RQ for carbohydrates (typically 0.77–1.11) (Hilman et al., 2022). As the oxidation of CaOx produces two moles of CO_2 per mol O_2 consumed, an ARQ value of almost double that of typical respiration signals may be expected in soils where oxalotrophy is a dominant process (ARQ ~ 2.0 from Reaction (2). Therefore, the measurement of CO_2 and O_2 concentrations in soil pore spaces may allow detection of oxalotrophy and estimation of kinetics of this process. However, ARQ values are sensitive to redox reactions (e.g. N-species transformation), changes in litter quality (mineralization of relatively more oxidized or reduced C substrates) and microbial carbon use efficiency (CUE) (Angert et al., 2015; Hilman et al., 2022; Hodges et al., 2019; Smart et al., 2025) It has not been established whether OCP or other biogeochemical processes control ARQ values in termite-affected soils of South Africa.

Termites are a keystone species in warmer climatic regions (Jouquet et al., 2016) and are often referred to as 'soil engineers' due to their critical role in litter decomposition and soil bioturbation (Bottinelli et al., 2015; Cheik et al., 2019). Ecosystems of the Greater Cape Floristic Region are undergoing loss of biodiversity due to crop agriculture, livestock grazing and mining (Desmet, 2007), which removes the natural food source for termites. Cultivation has been shown to decrease topsoil organic C stocks of *heuweltjies* relative to uncultivated mounds (Sakala, 2023). It is not clear whether large-scale removal of oxalate-containing indigenous vegetation, which is ongoing in the Swartland region where *heuweltjies* occur (Halpern & Meadows, 2013), reduces the overall capacity of *heuweltjie* soils to sequester C via the OCP. Understanding the factors controlling the extent and rate of OCP in termite-affected soils is crucial to exploit this process of C sequestration (Syed et al., 2020) and inform land-use decision-making, as we note that MICP is not currently recognized as an ecosystem service (ESS) (Görgen et al., 2021; Wang et al., 2023).

Assessing OCP-driven soil C sequestration is crucial for valuing dryland ESSs (Görgen et al., 2021; Wang et al., 2023). Decomposition and transformation pathways of CaOx-enriched organic material in termite-affected soils remain poorly understood, with key questions being: (i) what are the temporal changes in soil geochemical properties because of CaOx or frass addition and (ii) how sensitive is the OCP to vegetation disturbance due to land use changes such as intensive agriculture? The aim of this study was to examine the effects of CaOx or frass addition on biogeochemistry of soils from undisturbed and cultivated termite mounds. We monitored soil alkalinity, $CaCO_3$ stability, N-speciation and ARQ values in soils incubated for one week after addition

of pure CaOx or *M. viator* termite frass. We hypothesized that the OCP occurs to a lesser extent in cultivated termite mounds than in pristine mounds and that ARQ values reflect geochemical changes associated with the OCP.

2. Methods and materials

2.1. Site and samples

The soils were sampled on a farm outside the town of Koringberg in the Western Cape province of South Africa (Fig. 1). The main land use is winter rainfall crop rotations (oats, wheat, and annual medics) with periodic addition of lime and/ or fertilizer to the cultivated soils. The soils are Leptisols and Luvisols formed in binary parent material, which consist of aeolian deposits of the Quaternary Sandveld sediments overlying quartz-muscovite-biotite schist of the Mooreesburg Formation (Belcher, 2003). The local climate is warm-summer Mediterranean (Csb Köppen-Geiger classification), with mean annual rainfall of 435 mm and mean annual temperature of 17 °C (Swartland Area Information, n.d.). Soils formed in the landscape surrounding termite mounds are non-calcareous (Nel, 2024).

Approximately 30 kg of topsoil (up to depth of 20 cm) was collected from each of two selected *heuweltjies* in September 2023. One *heuweltjie* was in undisturbed indigenous renosterveld vegetation and the other was approximately 200 m away in a cultivated field where oats had been planted several weeks prior to sampling. Both *heuweltjies* had soil carbonates present, as confirmed using 10 % HCl. The *heuweltjies* in the renosterveld were dominated by succulent shrubs (e.g., *Euphorbia mauritanica*, *Euphorbia hamata*, *Aizoon sp*. and *Mesembryanthemum* cf. *longistylum*) and surrounding soils were dominated by low shrubs (e.g., *Eriocephalus africanus*, *Aspalathus acuminata* and *Calobota cytisoides*) (Vermonti, 2022).

Excavation of a deep trench through each *heuweltjie* revealed visible layers of pedogenic carbonates in both mounds. The cultivated mound was larger, more dome-shaped and showed stronger morphological expressions of carbonates (Bk and Bkm horizons), whereas the uncultivated mound was smaller and displayed weaker carbonate features, such as coatings beneath rock clasts and carbonates disseminated within the soil matrix, as observed by a weak reaction with 10 % HCl. The pH of the cultivated mound soil was also higher than that of the uncultivated mound soil (Table 1) and could be attributed to addition of agricultural lime or the greater degree of leaching of the higher lying uncultivated mounds. *Heuweltjie* soil samples were collected from the trench walls using cores of a known volume for bulk density determination. Soils from each *heuweltjie* were dried at 40 °C, sieved at 2 mm diameter mesh, and homogenized by agitation. The bulk density and gravel content of the soils were evaluated by weighing cores of known volume before and after sieving. Soil texture was evaluated in-field by the field method (Thien, 1979).

Termite frass volumes and termite-related features (e.g., foraging activity, bioturbation) were more abundant near uncultivated *heuweltjies* than cultivated ones. In the cultivated field, termites were observed feeding on crop residues. Approximately 5 kg fresh termite frass was collected from the cultivated field and from the undisturbed area. Frass samples from each of the two areas (cultivated and

Table 1
Location of soil sampling sites in cultivated and uncultivated fields and general topsoil (0–20 cm depth) physicochemical properties.

Longitude	Latitude	Disturbance level	Texture class	pH
18.64209	–33.00840	Uncultivated	Loamy sand	6.62
18.64424	–33.00866	Cultivated	Sandy loam	7.18

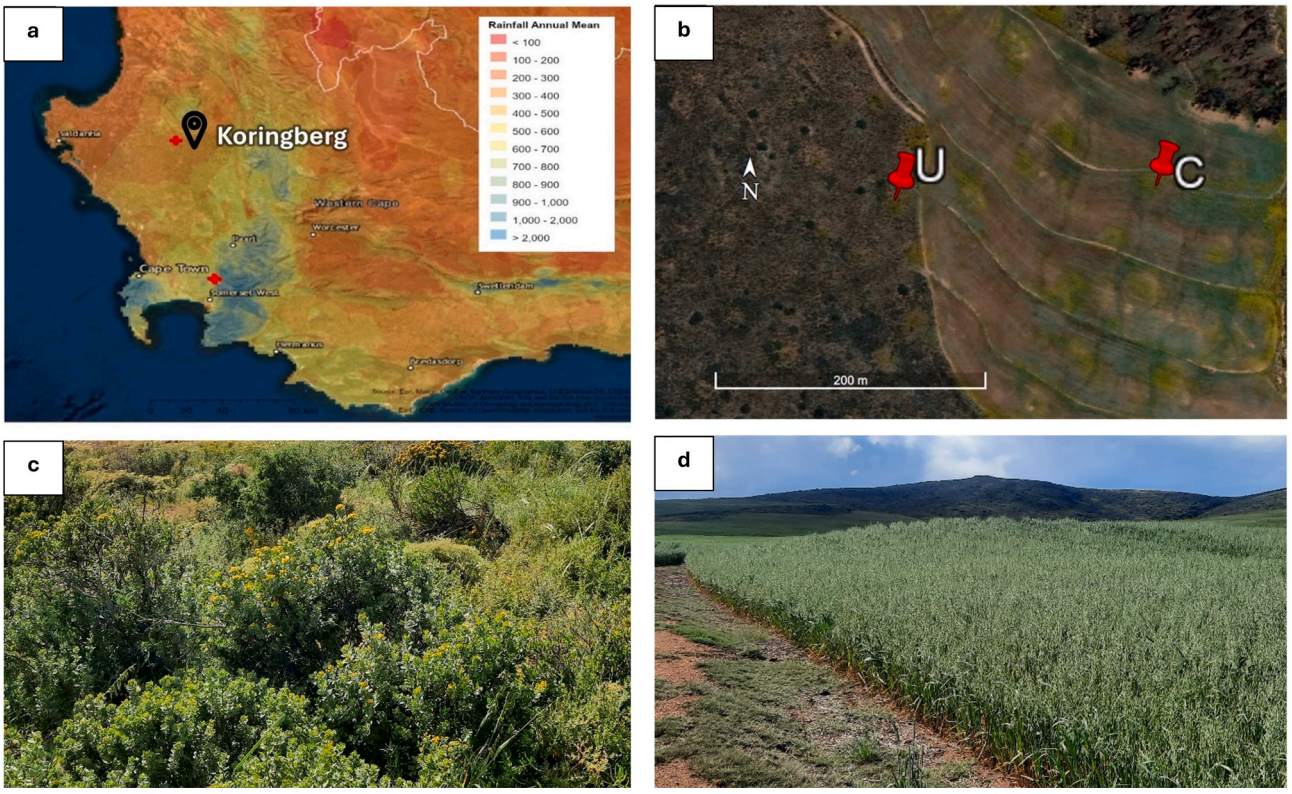

Fig. 1. A: location of sampling site in koringberg in the country of south africa. b: aerial satellite image showing sampling locations of heuweltjies in the indigenous renosterveld (u) and the cultivated field (c); geographical coordinates of the two locations are–33.00840, 18.64209 and –33.00866, 18.64424 respectively. Image retrieved from CapeFarmMapper 3 on 24 April 2024 at URL: https://gis.elsenburg.com/apps/cfm/. c: Indigenous renosterveld vegetation in Koringberg. d: Termite mound in a cultivated field in Koringberg, South Africa. Photos by Teneille Nel.

uncultivated) were air-dried, sieved through 2 mm diameter mesh, and thoroughly mixed. The CaOx content of homogenized frass samples from both disturbance-levels were determined by infrared spectroscopic analysis of dried, ball-milled sub-samples of approximately 1 g (analyses performed in triplicate i.e., on 3 different sub-samples for each disturbance-level) (Nel et al. 2025, in press). Frass from uncultivated *heuweltjies* exhibited higher EC and greater concentrations of DOC, TOC, CaOx, active NH_4^+, and water-extractable cations (Ca^{2+}, Mg^{2+}, Na^+, and K^+) than frass from cultivated mounds (Table 2). TIC and NO_3^- levels were negligible, and both cultivated and uncultivated frass samples showed high C:N ratios.

2.2. Incubation procedure

The homogenized soils were split into 9 microcosms for both levels of disturbance (cultivated and uncultivated), each with three substrate treatments applied in triplicate (Supplementary Information Figure S1a). For each microcosm, 2 kg soil was placed in a sterilized 4 L container (Supplementary Information Figure S1b) with a perforated lid to allow gas exchange with the atmosphere. The open-system design avoids disturbance of gas diffusion gradients between the soil and atmosphere as well as over- or under-pressurization of the headspace which is a common source of gas composition measurement error in chamber-based systems (Davidson et al., 2002).

The three treatments were the control (soil only), addition of termite frass, and addition of pure analytical-grade CaOx (Thermo Fisher Scientific Inc., United States). CaOx was applied at a rate of 3.587 mg g^{-1} soil, equivalent to 0.025 mmol g^{-1} soil. The frass collected from the uncultivated field (CaOx content of 0.07 mmol g-1) was applied to uncultivated soils at a rate of 0.4 g frass g^{-1} soil, which is equivalent to the rate of 0.028 mmol CaOx g^{-1} soil. Frass from the cultivated wheat field (CaOx content of 0.04 mmol g^{-1}) was applied at the same mass-based rate as the uncultivated frass treatment (0.4 g frass g-1 soil), resulting in a lower equivalent CaOx application of 0.016 mmol g^{-1} soil. The application rates were determined based on preliminary experiments (data not shown) using simple C substrates such as glucose and oxalic acid. The optimal concentration was defined as the amount that triggered the highest respiration rate by the third day of incubation, beyond which no further increase in respiration was observed. This concentration was then reduced to ensure that the volume of frass needed to match the equivalent CaOx application rate did not exceed the soil volume.

After the manual mixing of supplements and soils for each microcosm, incubations were immediately initiated by moistening soils with the volume of distilled water required to bring soils to 50 % water-filled pore space (Franzluebbers, 2021) which was pre-determined for both soil and soil-frass mixtures. The time-zero soil sampling was performed after initial mixing and addition of water (duration of two hours). The incubation took place at ambient conditions (average room temperature of 19 °C). Soil chemical properties as well as soil pore gas composition was monitored for one week.

Table 2
Chemical properties of frass samples from cultivated and uncultivated heuweltjies.

Disturbance level	Uncultivated	Cultivated
pH	7.4 ± 0.08	7.5 ± 0.03
EC (μS cm^{-1})	4373 ± 561	1250 ± 139
Na^+ (ug g^{-1})	2494 ± 696	505 ± 126
K (ug g^{-1})	1576 ± 444	940 ± 254
Mg^{2+} (ug g^{-1})	621 ± 169	172 ± 27.5
Ca (ug g^{-1})	428 ± 96.3	275 ± 54.9
DOC (mg g^{-1})	3 ± 0.800	0.8 ± 0.386
DIC (ug g^{-1})	24.2 ± 11.2	22 ± 8.08
TOC (%)	26.97 ± 2.16	17.6 ± 0.50
NH_4^+ (ug g^{-1})	17.3 ± 1.65	8.1 ± 0.362
C: N	34.56 ± 3.51	35.67 ± 6.53
CaOx (mmol g^{-1})	0.0714 ± 0.0017	0.0439 ± 0.0008

2.3. Chemical analyses

Preliminary analyses showed that the greatest changes in geochemical parameters occurred within the first three days of the incubation period. The measurement of CO_2 flush for three days following rewetting of dried soil is a standard indicator of biological activity and is sensitive to changes in soil management in addition to having strong correlation with longer term effects (Franzluebbers, 2021). Soil samples were harvested from each microcosm at time zero, on day three and the final day of the incubation period. Each microcosm was sampled by coring the entire depth of the soil in the incubation container (core i.d. 3.5 cm). Samples were taken from adjacent areas in each container on subsequent sampling days and dried for a minimum of 12 h at 60°C before performing chemical analyses.

The pH, electrical conductivity (EC) and water-soluble cation and anion concentrations of the soil samples were determined as follows. Each soil sample (10 g) was shaken in 20 mL distilled water for 30 min at 450 rpm (LABsmart) and centrifuged for 5 min at 3000 rpm (Zonkia SC-3612). The pH of the supernatant was measured using a Metrohm 914 pH meter (Metrohm, Herisau, Switzerland) and EC of the supernatant was measured using a Jenway 4510 Conductivity Meter (Jenway, England). The extract was then clarified by passing it through a 0.45 μm mesh diameter cellulose acetate membrane filter and 10 mL of the filtrate was diluted 5x in distilled water and frozen for up to 36 h before quantitative analysis of water-soluble cations (Ca^{2+}, Mg^{2+}, Na^+ and K^+) and anions (Cl^-, NO_3^-, PO_4^{3-}, SO_4^{2-}) by ion chromatography using a Metrohm 930 Compact IC Flex oven (Metrohm, Herisau, Switzerland).

The dissolved organic carbon (DOC) and DIC contents of soil leachates were determined by analysis of dilute salt extracts (Chantigny & Angers, 2008) as follows. Soil samples were processed as described above except for the use of 5 mM $CaCl_2$ (Merck, Germany) instead of water, before quantitative analysis of total dissolved C using an Elementar vario TOC cube (Elementar, Germany) as well as DOC after removal of DIC by acidification. The DIC content of the extract was calculated as the difference between the total dissolved carbon and DOC content. The DIC is a measure of the dissolved carbonates, mainly in the form of bicarbonate (HCO_3^-) (Cole & Prairie, 2014).

The mineralized (active) inorganic nitrogen (N) concentration of the soil samples was determined by analysis of concentrated salt extracts (Mulvaney, 2018). Each soil sample (7 g) was shaken in 70 mL concentrated salt solution (2 M KCl, Kimix, South Africa) for 1 h at 200 rpm (LABsmart) and allowed to settle for 1 h. The extract was then filtered through funnels lined with Whatman 41 filter paper (GE Healthcare Life Sciences, United States) and immediately analysed for total oxidized N (TON), nitrite (NO_2^-)-N and ammonium (NH_4^+)-N using a Skalar BLUVISION discrete analyser (Skalar Analytical, The Netherlands). The nitrate (NO_3^-)-N concentrations were calculated as the difference between the TON and (NO_2^-)-N content. The cation, anion, DOC, DIC, TON, NO_2^- and NH_4^+ concentrations of blank, filtered 2 M KCl extract (one extract per analysis type) were also measured and subtracted from the measured sample values; the concentrations of potential contaminants were negligible.

Sub-samples of each soil sample were ball-milled for analysis of total C by combustion using an Elementar Vario Macro Cube CN (Elementar GmbH, Germany) as well as total organic carbon (TOC) after removal of total inorganic C (TIC) by acidification with 3 % HCl in foil capsules (500 μL: 100 mg soil, evaporated for 12 h in a fume hood). The TIC content of each soil sample was calculated as the difference between the total C and TOC. This TIC is assumed to represent mineral carbonate mainly in the form of $CaCO_3$ (Doner & Lynn, 1989). Three sub-samples of each of the two homogenized frass samples used as cultivated- and uncultivated-level supplements were subjected to the same chemical analyses as for soil samples. The CaOx content of frass samples was reported (Section 2.1), but CaOx concentrations in soils were below the detection limit of 8.4μmol g^{-1} (data not shown). We compared replicates of the homogenized frass samples to demonstrate the difference

between these supplements and highlight reproducibility of the composition of frass samples administered to different biological replicates.

2.4. Gas monitoring

The gas sampling system is illustrated in Supplementary Information Figure S2. Soil pore gas samples were taken from each microcosm through a 0.5 cm diameter hole drilled into the side of a stainless-steel tube (inner diameter 6.35 mm, outer diameter 7.24 mm) at 1 cm from the lower end of the tube. Each tube was inserted vertically into the soil, entering at the centre of the circular surface of the microcosm. The composition of soil CO_2 and O_2 gas in each microcosm was measured successively every 12 h for 5 min at a flow rate of 50 mL min^{-1} by a Sable Foxbox gas analyzer (Gallagher & Breecker, 2020). The sampling of gases and recording of gas composition once per second for the sampling duration was automated with a BX-DM1E-M programmable logic controller (PLC) using Do-More Designer software (Automation Direct). The flow of gas was directed from each microcosm via Bev-a-line tubing (inner diameter 3.2. mm, outer diameter 6.4 mm) connected to a manifold of solenoid valves and passed through a column of magnesium perchlorate (Industrial Analytical, South Africa) to remove water vapour before reaching the detector. Each microcosm gas measurement was preceded by sampling of atmospheric air via the manifold for 3 min at a flow rate of 50 mL min^{-1} to provide a baseline for comparison with the soil pore gas composition.

2.5. Data analyses

Data analyses were conducted in the R computing environment (RStudio Team, 2019). The average soil geochemical measures (pH, EC, water-soluble cations, DOC, DIC, NH_4^+-N, NO_3^--N, NO_2^--N, TOC, and TIC) of triplicate microcosm sets i.e., for each of the substrate treatment-disturbance level combinations were calculated for each measurement period. The effects of disturbance level and substrate treatments on initial pH measurements of microcosm soils were tested by performing two-way Anova and post-hoc Tukey tests for replicated block data.

Geochemical data from soil water extracts (Supplementary Information Table S1) and laboratory temperatures (Ambient Weather WS-2902D) were used to calculate solute speciation, ion activities, and calcite saturation indices with PHREEQC (v3.7.3) using aqueous models from the PHREEQC.dat database (raw input and output files available online at https://doi.org/10.17632/mksk4tc5yk.1). Carbonate alkalinity was simulated as organic acids complicate titration-based measurements (Drever, 1997). PCO_2 was modelled using DIC, pH, and modelled chemical data. Simulated alkalinity, derived from selected ion data, enabled relative treatment comparisons but did not represent true total alkalinity.

Pre-processing of the measured CO_2 and O_2 concentrations was required for data interpretation (Fig. 3). The raw values versus time yielded spectra-like plots where the baseline represented atmospheric gas composition, and the peaks represented pore space gas from individual microcosms that were sampled sequentially. The baseline of the O_2 time-series data was observed to drift (this may be attributed to temperature or water vapour effects on the hydrogen fuel cell detector of the gas analyzer (Liland *et al.*, 2023). Baseline drift was corrected using a rolling ball algorithm (width of local window for maximization and for smoothing = 200 with x-axis units in seconds with a resolution of 1) (Cooper *et al.*, 2006). Peak values (microcosm gas concentrations) relative to atmosphere were used to calculate CO_2 produced and O_2 consumed of each microcosm at each measurement time throughout the incubation. The peaks were detected by applying a local regression algorithm (span = 0.0005) and smoothing by resampling followed by isolation of local maxima (half-width = 200) using the "argmax" function (Huber, 2012). The mean peak values were obtained by averaging y-values over a 40-second measurement interval centred around each detected maximum. This allowed accounting for uncertainty of the measurement due to noise in the signal. The ARQ value corresponding to CO_2/ O_2 concentrations of every microcosm was calculated for each measurement period according to Equation (6). The average gas concentrations and ARQ-values of triplicate microcosm sets i.e., for each of the treatment-level combinations, were calculated for each measurement period. Low flow rates observed on the fourth day of measurement were likely due to soil particles blocking the tubes. Flow rates returned to normal except for cultivated frass and one CaOx treatment, where low flow persisted during the first measurement. Gas data from these instances were excluded (Supplementary Information Table S2).

The changes in soil geochemical properties and ARQ values for each of the treatment-level combinations were calculated as the difference between the values measured on the third day and the first day. The changes in measured values over the first three days were indicated as delta ("d") values, with the letter "d" added as prefix to the property of interest. The effects of disturbance level and substrate treatments on the changes in chemical properties over three days were tested by performing two-way Anova and post-hoc Tukey tests for replicated block data. For parameters with heteroscedastic variance among comparison groups (Levene's test, $p < 0.05$), the changes in chemical parameters were compared by Welch adjusted means Anova and post-hoc tests (RStudio Team, 2019). Inspection of dARQ probability distributions revealed outlier data points. Winsorizing (Dixon, 1960) was applied to dARQ data using the "scores" function with the "irq" option (Komsta, 2022). The Kenward-Roger approximation for a linear mixed model type III Anova (Bates et al., 2015) and post-hoc least significant differences (LSD) (Lenth, 2016) test was conducted to test the effects of treatments, levels, and their interactions on the dARQ.

Principal component analysis (PCA) of the changes in chemical properties over three days was performed using the "prcomp" function (RStudio Team, 2019). A scree plot was used as a basis to select principal components (PCs) explaining variation of chemical properties of the samples. We constructed PCA biplots showing the contribution of chemical parameters to the two PCs that explained the greatest proportion of variance (Supplementary Information Figure S3).

3. Results

3.1. Carbon and nitrogen content

Changes in soil chemical parameters over one week are presented in Figs. 2 and 3 and Supplementary Information Figures S5-S9. All raw statistical analysis results are available online (https://doi.org/10.17632/mksk4tc5yk.1).

Total C content of uncultivated soils was consistently greater than that of cultivated soils (Supplementary Information Figure S5). Increases in total C of the frass treatments within the first three days of incubation ($dC = 1.505 \pm 1.04$ %) were greater than for the other treatments. TIC concentrations decreased in most microcosms, with a more significant decrease in uncultivated soils ($dTIC = -0.105 \pm 0.15$ %) than in cultivated soils (Fig. 2a). Initial TOC in frass-treated soils increased after three days but declined by day seven (Fig. 2b). DIC concentrations increased through time in all treatments, with the largest increase in frass-treated soils ($dDIC = 2.59 \pm 1.21$ μg g^{-1} soil, Fig. 2c). DOC content decreased most significantly in the uncultivated frass treatment within three days (-0.1824 ± 0.079 mg g^{-1} soil, Fig. 2d).

Increase in active NO_2^- and concomitant decrease in active NO_3^- was observed in the control and CaOx treatments (Supplementary Information Figure S6a and c). Active NH_4^+ decreased over one week in most treatments (Supplementary Information Figure S6b), with the greatest decrease in NH_4^+ within the first three days observed in the uncultivated frass treatment ($dNH_4^+ = -11.12 \pm 0.51$μg g^{-1} soil).

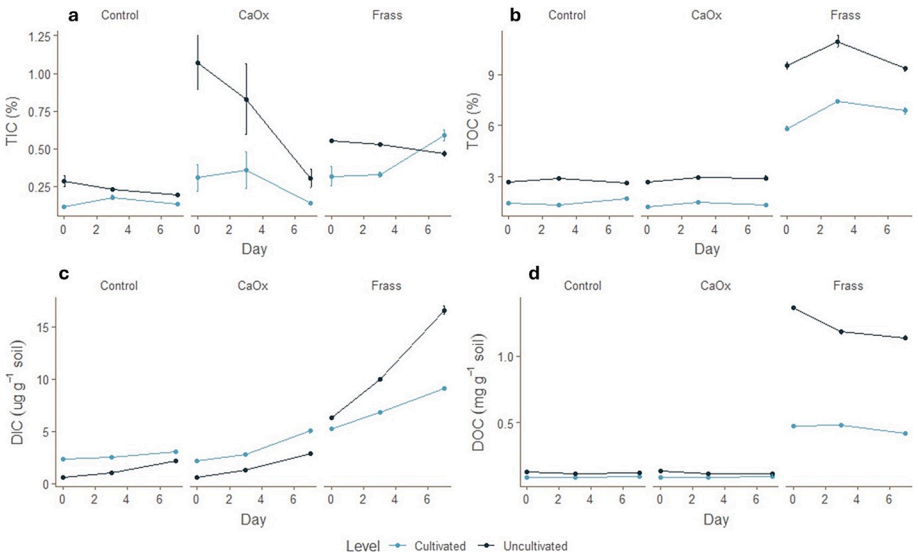

Fig. 2. Total inorganic carbon (TIC, a), total organic carbon (TOC, b), dissolved inorganic carbon (DIC, c) and dissolved organic carbon (DOC, d) of microcosm soils with different substrate treatments (calcium oxalate i.e., CaOx, termite frass and a control) and disturbance levels (cultivated and uncultivated) on three days during one week of incubation. Bars indicate standard error of measurement (SE) for triplicate measurements (biological replicates).

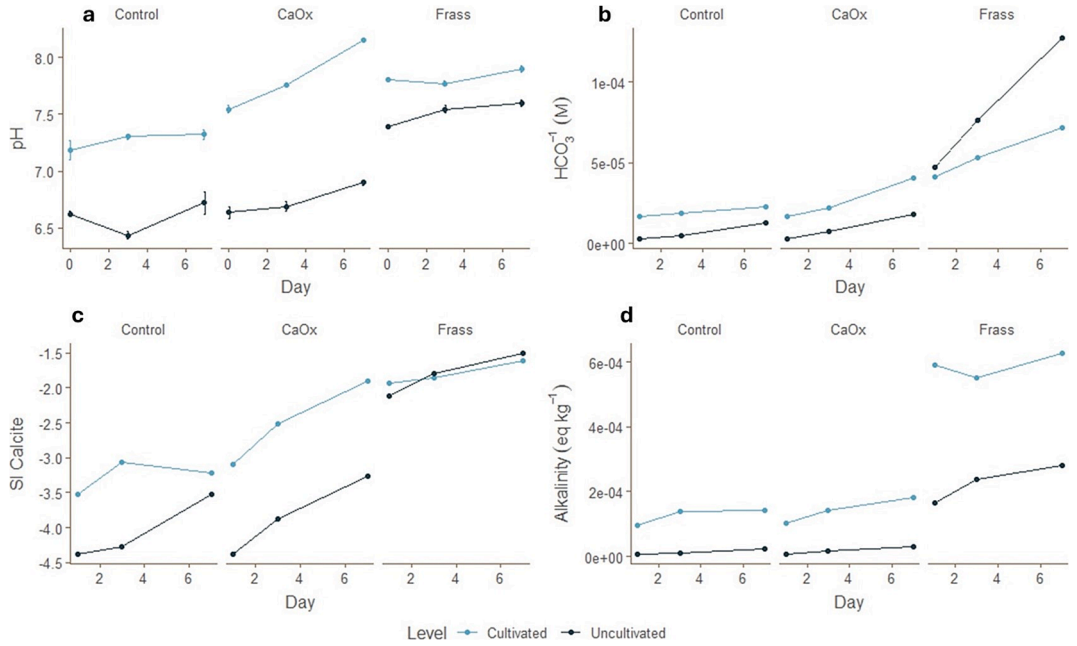

Fig. 3. Soil pH (a), simulated log activity of bicarbonate (HCO_3^-) (b), simulated saturation index (SI) of calcite (c) and simulated carbonate alkalinity (d) in microcosms with different substrate treatments (calcium oxalate i.e., CaOx, termite frass and a control) and disturbance levels (cultivated and uncultivated) over one week. Bars in panel (a) indicate standard error of measurement (SE) for triplicate measurements (biological replicates).

3.2. Aqueous chemistry

Initial concentrations of water-soluble cations were higher in uncultivated soils and frass-treated soils compared to other treatments (Supplementary Information Figure S7). Water-soluble Ca^{2+}, Mg^{2+}, Na^+, and K^+ levels decreased after three days in uncultivated soils treated with frass. Conversely, water-soluble Ca^{2+} levels increased in uncultivated control and CaOx treatments throughout the incubation.

Initial pH was higher in frass treatments (7.60 ± 0.23) compared to other treatments and higher in cultivated soils (7.51 ± 0.30) than uncultivated soils (6.88 ± 0.38) (Fig. 3). A significant pH increase (dpH = 0.213) was observed in the cultivated CaOx-treated soil compared to the frass-treated soil. After seven days, the pH of the cultivated CaOx treatment increased by 0.49 ± 0.12 units (Fig. 3).

Simulated HCO_3^- concentrations increased in all microcosms throughout the incubation, with the greatest increase in the uncultivated frass treatment (0.0799 mM) (Fig. 3). All microcosm soil samples were undersaturated with respect to calcite, however, values in a saturated paste would have been higher than these than those measured in this study, as we used a 1: 2 soil: solution ratio for leaching, which is more dilute. Initial calcite saturation indices (SI) were higher in frass treatments, increasing over time, with the largest increase in CaOx-treated soils (1.19 units) (Fig. 3). Simulated carbonate alkalinity increased across all treatments, with the cultivated frass treatment showing notably higher values (mean carbonate alkalinity of 0.59 meq L^{-1} over seven days). The uncultivated frass treatment had the greatest net

increase in simulated carbonate alkalinity (0.118 meq L-1) (Fig. 3).

3.3. Principal component analysis

PCA biplots (Supplementary Information Figure S8) illustrate variation in the dataset grouped by disturbance level and treatment. Key variables contributing to variation were dDIC, dN, and dTOC for PC1 and dNO_3^-, dTIC, and dpH for PC2 (Supplementary Information Table S3). PC1 differentiated treatments, showing distinct chemical changes in frass-treated soils compared to control and CaOx treatments, with DIC, TOC, and dN explaining more variation in frass-treated soils.

3.4. Respiratory gas composition

The CO_2 production, O_2 consumption and ARQ values of the control, CaOx and frass-treated soils during one week of incubation are shown in Supplementary Information Figure S9. The highest CO_2 production and O_2 consumption occurred during the first three days. CO_2 production was over 100 times greater in the frass treatment than in the control and over 80 times greater than in the CaOx treatment. Similarly, O_2 consumption was more than 170 times greater in frass treatments compared to the control and over 150 times greater than in CaOx treatments. The ARQ values of the control and CaOx treatments (mean ARQ of 1.3 over one week for both treatments) were higher than values expected in soils where metabolism of simple carbohydrates dominate the microbial respiratory signal (Hodges *et al.*, 2019a). CaOx treatments exhibited higher ARQ values on days 3 and 6–7. ARQ decreased during the first three days in uncultivated control (-0.14 ± 0.07) and frass treatments (-0.05 ± 0.14).

4. Discussion

4.1. Effect of cultivation

Our study presents the first comparison of termite frass chemistry from cultivated and uncultivated fields. Frass from termites feeding on indigenous vegetation had higher salinity, water-extractable cations, CaOx, DOC, and NH_4^+ content than frass from cultivated fields (Table 2). This likely reflects differences in termite diets, with indigenous renosterveld vegetation versus crop residues (Clarke et al., 2023; Vermonti et al., 2025). Cultivation influences frass composition, potentially altering *heuweltjie* soil biogeochemistry.

Differences in frass chemistry affected soil microbial activity, with greater CO_2 production and O_2 consumption in uncultivated frass treatments, which declined more rapidly over time (Supplementary Information FigureS9). This suggests enhanced microbial respiration due to greater nutrient content of frass from uncultivated fields, followed by microbial senescence (Parzych & Klionsky, 2014; Vázquez-Vuelvas et al., 2021). The greater DOC decrease in uncultivated frass compared to the cultivated frass treatment (Fig. 3, 13 % in three days) indicates higher microbial uptake (Dilly, 2003). Higher total C accumulation in cultivated treatments (Supplementary Fig. S5) suggests greater microbial CO_2-fixation, though the mechanism remains unclear.

Microbial biomass is an important store of soil C (Smart et al., 2025). Frass nutrients and microbial load possibly stimulated biomass production, with a 20 % TOC increase in frass treatments within three days (Fig. 2). Changes in N, an essential nutrient required by microorganisms for biomass production (Masiello et al., 2008), were most prominent in the uncultivated frass-treated soils (Supplementary Information Figure S8). The decrease in NO_3^- content (Supplementary Information Figure S6c) may be explained by dissimilatory nitrate reduction, which is favoured by the high C:N ratio of frass (Li et al., 2020). The NH_4^+ produced by this reaction would be readily available for assimilation by the microbial community. The greater decrease in active NH_4^+ content in the uncultivated frass treatment (Supplementary Information Figure S6b) may indicate less microbial N uptake in the cultivated frass-treated soil. Therefore, cultivation may have indirect effects on soil C stocks due to the influence of vegetation change on nutrient quality of termite frass, subsequently impacting microbial biomass production.

ARQ values were higher in uncultivated CaOx-treated soils compared to their cultivated counterparts on days 3, 6 and 7 (Supplementary Information Figure S9), which may indicate a greater dominance of oxalotrophy in uncultivated versus cultivated soils. Alternatively, greater ARQ values in uncultivated soil may be a result of higher CUE, as microbial uptake of nitrate associated with anabolism decreases net O_2 consumption relative to respiration without biomass production (Smart et al., 2025). A third possible explanation of ARQ differences between disturbance levels of CaOx-treated soils, is metabolism of compounds with lower RQ (closer to 1.0) in cultivated soil versus uncultivated soil, potentially due to destabilization of pre-existing SOM by oxalic acid (priming effect). Oxalic acid addition was shown to increase mineralization of mineral-associated organic matter (Jilling et al., 2021), but labile C was preferentially metabolized when available (Georges Martial et al., 2023). This implies that uncultivated soil may have greater availability of labile SOC compared to cultivated soils.

Our study underscores the value of monitoring soil pore gas composition to reveal microbial functions under distinct land uses and substrate treatments. However, this method has limitations when applied to complex substrates like termite frass. The ARQ differences between cultivated and uncultivated CaOx-treated soils indicate that cultivation reduced the extent of oxalotrophy, microbial CUE or labile C availability in termite mound soil. Replication across different *heuweltjies* and further microbiological analyses are needed to confirm these results. A comprehensive summary of factors affecting ARQ is provided in Supplementary Information Table S4.

4.2. Evidence of oxalotrophy

Bicarbonate alkalinity is a simple but non-specific indicator of oxalotrophy, as HCO_3^- is produced during oxalate oxidation, with concomitant proton consumption leading to pH increases (Cailleau et al., 2014; Gatz-Miller et al., 2022; Rowley et al., 2017). We investigated ARQ as an oxalotrophy indicator by linking soil pore gas composition to chemistry in CaOx-incubated soils.

Increases in pH, calcite SI (Fig. 3), and DIC (Fig. 2) in CaOx and frass treatments suggest the OCP, though organic salts in frass, especially Na^+ salts, may also contribute to soil alkalinity (Z.-A. Li et al., 2008). The smaller pH and calcite SI increases in frass-treated soils over time (Fig. 3) may be attributed to buffering by organic acids. Uncultivated frass-treated soils showed the largest increase in simulated HCO_3^- concentrations (Fig. 3b). The 44.7 % increase in DIC in frass treatments (Fig. 2) suggests microbial transformation of organic C into dissolved carbonate species. Slight increases in DIC of control and CaOx treatments may also be attributed to dissolution of respired CO_2 in water but increases in dissolved Ca^{2+} in these microcosms (Supplementary Information S. 7a) suggest that calcite dissolution may have occurred. Alternatively, CaOx dissociation is another potential cause of increases in dissolved Ca^{2+}. A decrease in water-soluble Ca^{2+} in the uncultivated frass treatment (Supplementary Information S. 7a) may have resulted from Ca precipitation, microbial uptake or sorption of Ca by frass.

Higher initial pH in cultivated mound soil (7.18) than in uncultivated soil (6.62) (Table 1) likely reflects agricultural lime application, but carbonate accumulation due to topography may also play a role (see Section 2.1 Site and samples). In cultivated soils, frass and CaOx treatments had a higher initial pH than controls (0.5–0.7 units, Fig. 3a). Frass-treated soils showed the highest starting pH, likely due to alkalinity produced by organic salts in the frass (particularly Na^+ salts) (Li et al., 2008). This raised pH, along with higher initial Ca^{2+} and DIC content (Supplementary Figs. S7a, Fig. 2), raised initial calcite SI. The greatest pH and calcite SI increases occurred in cultivated CaOx treatments, indicating a stronger microbial response to CaOx addition than in

uncultivated soils.

ARQ values in CaOx treatments were less than or equal to ARQ values of the control, especially in uncultivated soils (Supplementary Information Figure S9). Therefore, ARQ trends did not clearly support the occurrence of the OCP. Instead, soil pore gas composition seems to have reflected other decomposition trends such as microbial CUE or labile C availability (see Section 4.1 Effects of cultivation). The ARQ increase on days 6–7 in both CaOx treatments and controls may indicate secondary metabolite metabolism after the exponential microbial growth phase (Andryukov et al., 2019; Seyedsayamdost, 2019).

The ARQ values of frass treatments also deviated from expected oxalotrophy patterns, with uncultivated frass-treated soils showing ARQ nearly 0.5 units lower than controls on day three (Supplementary Information Figure S9). This was likely due to respiration of reduced C forms like lignin (Angert et al., 2015; Hicks Pries et al., 2020; Hodges et al., 2019). Therefore, our results show that ARQ is not a suitable proxy for oxalotrophy in complex systems such as *heuweltjie* soils.

In summary, oxalotrophy may occur when CaOx is added to *heuweltjie* soils, but complex biogeochemical interactions complicate interpretations of soil pore gas measurements, especially in frass-treated soil. We find evidence of OCP as a potential C sequestration pathway in *heuweltjie* soils, but whether it is a dominant process cannot be concluded from this study.

4.3. Environmental significance

This study explores soil respiration and chemistry in oxalate-containing microcosms, with a schematic of termite-affected soil C cycling in Fig. 4. We demonstrate that *heuweltjies* are an important store of SIC formed by dissolution of microbially respired CO_2. Respiration activity was stimulated by nutrient-rich termite frass (Table 2), particularly in uncultivated treatments (Supplementary Fig S9). Termite tunnels in *heuweltjie* soils (Clarke et al., 2022; Francis et al., 2024) facilitate dissolved species transport to groundwater or the ocean for long-term storage (Taylor et al., 2016). $CaCO_3$ precipitates when the soil solution is supersaturated, which may also contribute to the stable SIC pool.

Microbial biomass could make an important contribution to C stores in *heuweltjie* soils, as nutrient-rich frass stimulated TOC increases (Fig. 2). Nitrogen transformations and NH_4^+ decreases (potentially attributed to microbial uptake) were most pronounced in uncultivated frass-treated soils (Supplementary Information S. 6). Therefore, lower nutrient content of termite frass in cultivated fields and resultant reduced microbial growth can have negative implications for SOC accumulation in *heuweltjies*.

The increase in total C in the uncultivated frass treatment (Supplementary Information Figure S5) implies microbial CO_2-fixation, possibly via autotrophic and heterotrophic pathways such as fungal nitrate assimilation or anaplerosis (Braun et al., 2021; Hou et al., 2011; X. Li et al., 2020). While CO_2 levels were elevated, fixation may have occurred near the surface, possibly stimulated by light entering through microcosm perforations (Gougoulias et al., 2014). Further research is needed to confirm CO_2-fixation mechanisms in termite-affected soils.

5. Conclusions

This work assessed the effects of land use change on soil C dynamics by a multi-proxy geochemical analytical approach. Our study presented indirect evidence of the OCP in termite-affected soils of the Greater Cape Floristic Region, such as increases in pH, calcite SI and inorganic C content. However, ARQ measurement proved unsuitable for assessing the OCP, and could not be used to confirm if oxalotrophy is a dominant pathway of C sequestration in *heuweltjie* soils.

Our study contributes valuable insights into potential factors that control soil pore gas composition and biogeochemistry in termite-affected soils. The greater degree of microbial activity in frass-treated soils compared to other treatments, especially in undisturbed *heuweltjies*, was attributed to greater nutrient availability in frass derived from indigenous vegetation. Our results suggest that cultivation can decrease C stocks in uncultivated *heuweltjie* soils due to SOM destabilization and/ or reduced microbial biomass production.

Indigenous vegetation of the region of study was shown to be a key component of SOC-SIC transformations in *heuweltjie* soils. Dissolved inorganic C produced (HCO_3^-) in *heuweltjies* due to dissolution of respired CO_2 in soil water may be leached to aquifers or precipitated as $CaCO_3$, thereby contributing to long-term C storage. Given their potential role in soil C sequestration and stabilization, termite-affected soils should be prioritized for conservation and further study as part of dryland

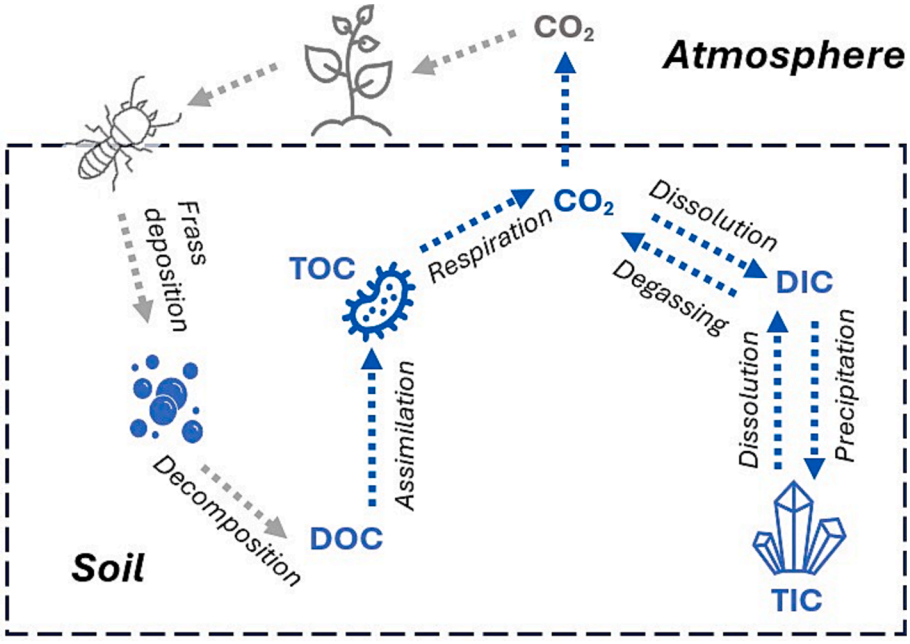

Fig. 4. Systems of carbon (CO_2: carbon dioxide, TOC: total organic carbon, TIC: total inorganic carbon, DOC: dissolved organic carbon, DIC: dissolved inorganic carbon) cycling that occurs in termite-affected soils Grey-coloured components occur in-situ but are not present in microcosms.

ecosystem services supporting climate regulation.

CRediT authorship contribution statement

Teneille Nel: Writing – original draft, Visualization, Project administration, Methodology, Investigation, Formal analysis, Data curation. **Catherine E. Clarke:** Writing – review & editing, Supervision, Project administration, Funding acquisition, Conceptualization. **Michele L. Francis:** Writing – review & editing, Investigation. **Darya Babenko:** Writing – review & editing, Investigation, Data curation. **Alf Botha:** Writing – review & editing, Methodology, Investigation. **Daniel O. Breecker:** Writing – review & editing, Investigation. **Don A Cowan:** Writing – review & editing, Investigation. **Timothy Gallagher:** Writing – review & editing, Methodology, Investigation, Funding acquisition, Conceptualization. **Pedro Lebre:** Writing – review & editing, Investigation. **Joseph R. McAuliffe:** Writing – review & editing. **Alyssa N. Reinhardt:** Writing – review & editing, Investigation. **Marla Trindade:** Writing – review & editing, Investigation, Data curation.

Declaration of competing interest

The authors declare that they have no known competing financial interests or personal relationships that could have appeared to influence the work reported in this paper.

Acknowledgements

This work was supported by the NRF-NSF Biodiversity on a Changing Planet program (National Science Foundation, United States: grant number 2224993 and National Research Foundation, South Africa: grant number 150452). We thank Stellenbosch University, South Africa, the Skye Foundation, South Africa and the National Research Foundation, South Africa for bursary provision. We acknowledge the Biogeochemistry Research Infrastructure Program (BIOGRIP), South Africa for sample analysis.

Appendix A. Supplementary data

Supplementary data to this article can be found online at https://doi.org/10.1016/j.catena.2025.108947.

Data availability

The data that support the findings of this study are available upon request.

References

Andryukov, B., Mikhailov, V., Besednova, N., 2019. The biotechnological potential of secondary metabolites from marine bacteria. *Journal of Marine Science and Engineering* 7 (6), 176. https://doi.org/10.3390/jmse7060176.

Angert, A., Yakir, D., Rodeghiero, M., Preisler, Y., Davidson, E.A., Weiner, T., 2015. Using O_2 to study the relationships between soil CO_2 efflux and soil respiration. Biogeosciences 12 (7), 2089–2099. https://doi.org/10.5194/bg-12-2089-2015.

Bates, D., Mächler, M., Bolker, B., Walker, S., 2015. Fitting linear mixed-effects models using lme4. *J. Stat. Softw.* 67 (1), 1–48. https://doi.org/10.18637/jss.v067.i01.

Belcher, R.W., 2003. *Tectonostratigraphic evolution of the Swartland region and aspects of orogenic lode-gold mineralisation in the Pan-African Saldania belt.* South Africa [PhD]. Stellenbosch University, Western Cape.

Bergel, S.J., Carlson, P.E., Larson, T.E., Wood, C.T., Johnson, K.R., Banner, J.L., Breecker, D.O., 2017. Constraining the subsoil carbon source to cave-air CO_2 and speleothem calcite in central Texas. Geochim. Cosmochim. Acta 217, 112–127. https://doi.org/10.1016/j.gca.2017.08.017.

Bottinelli, N., Jouquet, P., Capowiez, Y., Podwojewski, P., Grimaldi, M., Peng, X., 2015. Why is the influence of soil macrofauna on soil structure only considered by soil ecologists? *Soil Tillage Res.* 146 (PA), 118–124. https://doi.org/10.1016/j.still.2014.01.007.

Braun, A., Spona-Friedl, M., Avramov, M., Elsner, M., Baltar, F., Reinthaler, T., Herndl, G.J., Griebler, C., 2021. Reviews and syntheses: Heterotrophic fixation of inorganic carbon – significant but invisible flux in environmental carbon cycling. *Biogeosciences* 18 (12), 3689–3700. https://doi.org/10.5194/bg-18-3689-2021.

Brecevic, L., Kralj, D., 2010. Factors influencing the formation of calcium oxalate hydrates in vitro*. *Med Vjesn* 42 (4), 127–136.

Cailleau, G., Mota, M., Bindschedler, S., Junier, P., Verrecchia, E.P., 2014. Detection of active oxalate-carbonate pathway ecosystems in the Amazon Basin: Global implications of a natural potential C sink. *Catena* 116, 132–141. https://doi.org/10.1016/j.catena.2013.12.017.

Certini, G., Corti, G., Ugolini, F.C., 2000. Vertical trends of oxalate concentration in two soils under *Abies alba* from Tuscany (Italy). J. Plant Nutr. Soil Sci. 163 (2), 173–177. https://doi.org/10.1002/(SICI)1522-2624(200004)163:2<173::AID-JPLN173>3.0.CO;2-H.

Chantigny, M.H., Angers, D.A., 2008. Extraction and characterization of dissolved organic matter. In: Carter, M.R., Gregorich, E.G. (Eds.), *Soil Sampling and Methods of Analysis*, 2nd ed. CRC Press, pp. 617–635.

Cheik, S., Shanbhag, R.R., Harit, A., Bottinelli, N., Sukumar, R., Jouquet, P., 2019. Linking termite feeding preferences and soil physical functioning in southern-indian woodlands. *Insects* 10 (1), 1–12. https://doi.org/10.3390/insects10010004.

Clarke, C.E., Francis, M.L., Sakala, B.J., Hattingh, M., Miller, J.A., 2023. Enhanced carbon storage in semi-arid soils through termite activity. *Catena* 232, 107373. https://doi.org/10.1016/j.catena.2023.107373.

Clarke, C.E., Vermooten, M., Watson, A., Hattingh, M., Miller, J.A., Francis, M.L., 2022. Downward migration of salts in termite-affected soils: Implications for groundwater salinization. *Geoderma* 413, 115747. https://doi.org/10.1016/j.geoderma.2022.115747.

Cole, J.J., Prairie, Y.T., 2014. Dissolved CO_2 in freshwater systems. In: *Reference Module in Earth Systems and Environmental Sciences*. Elsevier. https://doi.org/10.1016/B978-0-12-409548-9.09399-4.

Cowan, D.A., Babenko, D., Bird, R., Botha, A., Breecker, D.O., Clarke, C.E., Francis, M.L., Gallagher, T., Lebre, P.H., Nel, T., Potts, A.J., Trindade, M., Van Zyl, L., 2024. Oxalate and oxalotrophy: an environmental perspective. *Sustainable Microbiology*. https://doi.org/10.1093/sumbio/qvad004.

Dauer, J.M., Perakis, S.S., 2014. Calcium oxalate contribution to calcium cycling in forests of contrasting nutrient status. *For. Ecol. Manage.* 334, 64–73. https://doi.org/10.1016/j.foreco.2014.08.029.

Davidson, E.A., Savage, K., Verchot, L.V., Navarro, R., 2002. Minimizing artifacts and biases in chamber-based measurements of soil respiration. *Agric. For. Meteorol.* 113 (1-4), 21–37. https://doi.org/10.1016/S0168-1923(02)00100-4.

Desmet, P.G., 2007. Namaqualand—A brief overview of the physical and floristic environment. *J. Arid Environ.* 70 (4), 570–587. https://doi.org/10.1016/j.jaridenv.2006.11.019.

Dilly, O., 2001. Microbial respiratory quotient during basal metabolism and after glucose amendment in soils and litter. *Soil Biol. Biochem.* 33 (1), 117–127. https://doi.org/10.1016/S0038-0717(00)00123-1.

Dilly, O., 2003. Regulation of the respiratory quotient of soil microbiota by availability of nutrients. *FEMS Microbiol. Ecol.* 43 (3), 375–381. https://doi.org/10.1016/S0168-6496(02)00437-3.

Dixon, W.J., 1960. Simplified estimation from censored normal samples. *Ann. Math. Stat.* 31 (2), 385–391. https://doi.org/10.1214/aoms/1177705900.

Doner, H.E., Lynn, W.C., 1989. Carbonate, halide, sulfate, and sulfide minerals. In: *SSSA Book Series*. Soil Science Society of America, pp. 279–330.

Drever, J.I., 1997. The carbonate system and pH control. In: *The Geochemistry of Natural Waters*. Prentice-Hall Inc.

Francis, M.L., Palcsu, L., Molnár, M., Kertész, T., Clarke, C.E., Miller, J.A., van Gend, J., 2024. Calcareous termite mounds in South Africa are ancient carbon reservoirs. *Sci. Total Environ.* 926, 171760. https://doi.org/10.1016/j.scitotenv.2024.171760.

Franzluebbers, A.J., 2021. Assessment and interpretation of soil-test biological activity. In: Karlen, D.L., Stott, D.E., Mikha, M.M. (Eds.), *Soil Health Series: Volume 2 Laboratory Methods for Soil Health Analysis*. John WIley & Sons, Inc | Soil Science Society of America Inc., pp. 126–151

Gadd, G.M., Bahri-Esfahani, J., Li, Q., Rhee, Y.J., Wei, Z., Fomina, M., Liang, X., 2014. Oxalate production by fungi: significance in geomycology, biodeterioration and bioremediation. *Fungal Biol. Rev.* 28 (2–3), 36–55. https://doi.org/10.1016/j.fbr.2014.05.001.

Gallagher, T.M., Breecker, D.O., 2020. The obscuring effects of calcite dissolution and formation on quantifying soil respiration. *Global Biogeochem. Cycles* 34 (12), 1–12. https://doi.org/10.1029/2020GB006584.

Garvie, L.A.J., 2006. Decay of cacti and carbon cycling. *Naturwissenschaften* 93 (3), 114–118. https://doi.org/10.1007/s00114-005-0069-7.

Gatz-Miller, H.S., Gérard, F., Verrecchia, E.P., Su, D., Mayer, K.U., 2022. Reactive transport modelling the oxalate-carbonate pathway of the Iroko tree: investigation of calcium and carbon sinks and sources. *Geoderma* 410 (December 2021). https://doi.org/10.1016/j.geoderma.2021.115665.

Görgen, S., Benzerara, K., Skouri-Panet, F., Gugger, M., Chauvat, F., Cassier-Chauvat, C., 2021. The diversity of molecular mechanisms of carbonate biomineralization by bacteria. *Discover Materials* 1 (1), 2. https://doi.org/10.1007/s43939-020-00001-9.

Gougoulias, C., Clark, J.M., Shaw, L.J., 2014. The role of soil microbes in the global carbon cycle: tracking the below-ground microbial processing of plant-derived carbon for manipulating carbon dynamics in agricultural systems. *J. Sci. Food Agric.* 94 (12), 2362–2371. https://doi.org/10.1002/jsfa.6577.

Groshans, G.R., Mikhailova, E.A., Post, C.J., Schlautman, M.A., Post, G.C., 2019. Valuation of soil inorganic carbon stocks in the contiguous United States based on the avoided social cost of carbon emissions. *Resources* 8 (119).

Halpern, A.B.W., Meadows, M.E., 2013. Fifty years of land use change in the Swartland, Western Cape, South Africa: characteristics, causes and consequences. *S. Afr. Geogr. J.* 95 (1), 38–49. https://doi.org/10.1080/03736245.2013.806101.

Harrison, R.B., Footen, P.W., Strahm, B.D., 2011. Deep soil horizons: contribution and importance to soil carbon pools and in assessing whole-ecosystem response to management and global change. *For. Sci.* 57 (1), 67–76.

Hervé, V., Junier, T., Bindschedler, S., Verrecchia, E., Junier, P., 2016. Diversity and ecology of oxalotrophic bacteria. *World J. Microbiol. Biotechnol.* 32 (2), 1–7. https://doi.org/10.1007/s11274-015-1982-3.

Hervé, V., Simon, A., Randevoson, F., Cailleau, G., Rajoelison, G., Razakamanarivo, H., Bindschedler, S., Verrecchia, E., Junier, P., 2021. Functional diversity of the litter-associated fungi from an oxalate–carbonate pathway ecosystem in Madagascar. *Microorganisms* 9 (5), 1–12. https://doi.org/10.3390/microorganisms9050985.

Hicks Pries, C., Angert, A., Castanha, C., Hilman, B., Torn, M.S., 2020. Using respiration quotients to track changing sources of soil respiration seasonally and with experimental warming. *Biogeosciences* 17 (12), 3045–3055. https://doi.org/10.5194/bg-17-3045-2020.

Hilman, B., Weiner, T., Haran, T., Masiello, C.A., Gao, X., Angert, A., 2022. The apparent respiratory quotient of soils and tree stems and the processes that control it. *J. Geophys. Res. Biogeo.* 127 (3). https://doi.org/10.1029/2021JG006676.

Hirt, H., Boukcim, H., Ducousso, M., Saad, M.M., 2023. Engineering carbon sequestration on arid lands. *Trends Plant Sci.* https://doi.org/10.1016/j.tplants.2023.08.009.

Hodges, C., Kim, H., Brantley, S.L., Kaye, J., 2019. Soil CO_2 and O_2 concentrations illuminate the relative importance of weathering and respiration to seasonal soil gas fluctuations. *Soil Sci. Soc. Am. J.* 83 (4), 1167–1180. https://doi.org/10.2136/sssaj2019.02.0049.

Hou, W., Lian, B., Zhang, X., 2011. CO_2 mineralization induced by fungal nitrate assimilation. Bioresour. Technol. 102 (2), 1562–1566. https://doi.org/10.1016/j.biortech.2010.08.080.

Jin, Z., Dong, Y., Wang, Y., Wei, X., Wang, Y., Cui, B., Zhou, W., 2014. Natural vegetation restoration is more beneficial to soil surface organic and inorganic carbon sequestration than tree plantation on the Loess Plateau of China. *Sci. Total Environ.* 485–486 (1), 615–623. https://doi.org/10.1016/j.scitotenv.2014.03.105.

Jouquet, P., Bottinelli, N., Shanbhag, R.R., Bourguignon, T., 2016. Termites: The neglected soil engineers of tropical soils. *Soil Sci.* 181 (March), 157–165. https://doi.org/10.1097/SS.0000000000000119.

Karabourniotis, G., Horner, H.T., Bresta, P., Nikolopoulos, D., Liakopoulos, G., 2020. New insights into the functions of carbon–calcium inclusions in plants. *New Phytol.* 228 (3), 845–854. https://doi.org/10.1111/nph.16763.

Komsta, L. (2022). *outliers: Tests for Outliers*. https://cran.r-project.org/package=outliers.

Kost, T., Stopnisek, N., Agnoli, K., Eberl, L., Weisskopf, L., 2014. Oxalotrophy, a widespread trait of plant-associated *Burkholderia* species, is involved in successful root colonization of lupin and maize by *Burkholderia phytofirmans*. Front. Microbiol. 4. https://doi.org/10.3389/fmicb.2013.00421.

Lal, R., Monger, C., Nave, L., Smith, P., 2021. The role of soil in regulation of climate. *Philos. Trans. R. Soc., B* 376 (1834). https://doi.org/10.1098/rstb.2021.0084.

Laudicina, V.A., Dazzi, C., Delgado, A., Barros, H., Scalenghe, R., Sim, U., 2021. Relief and calcium from gypsum as key factors for net inorganic carbon accumulation in soils of a semiarid Mediterranean environment. *Geoderma* 398.

Lenth, R.V., 2016. Least-squares means: the R package lsmeans. *J. Stat. Softw.* 69 (1). https://doi.org/10.18637/jss.v069.i01.

Li, X., Qian, W., Hou, L., Liu, M., Chen, Z., Tong, C., 2020. Soil organic carbon controls dissimilatory nitrate reduction to ammonium along a freshwater-oligohaline gradient of Min River Estuary, Southeast China. *Marine Pollution Bulletin* 160, 111696. https://doi.org/10.1016/j.marpolbul.2020.111696.

Li, Z.-A., Zou, B., Xia, H.-P., Ding, Y.-Z., Tan, W.-N., Fu, S.-L., 2008. Role of low-molecule-weight organic acids and their salts in regulating soil pH. *Pedosphere* 18 (2), 137–148. https://doi.org/10.1016/S1002-0160(08)60001-6.

Martin, G., Guggiari, M., Bravo, D., Zopfi, J., Cailleau, G., Aragno, M., Job, D., Verrecchia, E., Junier, P., 2012. Fungi, bacteria and soil pH: The oxalate-carbonate pathway as a model for metabolic interaction. *Environ. Microbiol.* 14 (11), 2960–2970. https://doi.org/10.1111/j.1462-2920.2012.02862.x.

Masiello, C.A., Gallagher, M.E., Randerson, J.T., Deco, R.M., Chadwick, O.A., 2008. Evaluating two experimental approaches for measuring ecosystem carbon oxidation state and oxidative ratio. *J. Geophys. Res. Biogeo.* 113 (3). https://doi.org/10.1029/2007JG000534.

McAuliffe, J.R., 2022. "Heuweltjies" – the "Little Hills" of western South Africa. In: Schmiedel, U., Oldeland, J., Finckh, H. (Eds.), Fairy circles of the namib desert: ecosystem engineering by subterranean social insects. Klaus Hess Verlag, pp. 302–339. https://doi.org/10.7809/b-e.00372.

McAuliffe, J.R., Hoffman, M.T., McFadden, L.D., Bell, W., Jack, S., King, M.P., Nixon, V., 2019. Landscape patterning created by the southern harvester termite, *Microhodotermes viator*: Spatial dispersion of colonies and alteration of soils. J. Arid Environ. 162 (July 2018), 26–34. https://doi.org/10.1016/j.jaridenv.2018.11.010.

Midgley, J.J., Harris, C., Harington, A., Potts, A.J., 2012. Geochemical perspective on origins and consequences of heuweltjie formation in the Southwestern Cape, South Africa. *S. Afr. J. Geol.* 115 (4), 577–588.

Midgley, J.J., Harris, C., Hesse, H., Swift, A., 2002. Heuweltjie age and vegetation change based on D13 C and 14 C analyses. *S. Afr. J. Sci.* 98, 202–204.

Misiewicz, B., & Vanwert, A. L. (2022). Analytical Methods for Oxalate Quantification: The Ubiqui-tous Organic Anion. 1–25. www.preprints.org.

Monger, C.H., Kraimer, R.A., Khresat, S., Cole, D.R., Wang, X., Wang, J., 2015. Sequestration of inorganic carbon in soil and groundwater. *Geology* 43 (5), 375–378. https://doi.org/10.1130/G36449.1.

Monger, H., Martinez-Rios, J., 2000. Inorganic carbon sequestration in grazing lands. In: *The Potential of U.S. Grazing Lands to Sequester Carbon and Mitigate the Greenhouse Effect*. CRC Press. https://doi.org/10.1201/9781420032468.ch4.

Nel, T., 2024. Termite-affected soils in the Western Cape – a toolkit for the assessment of oxalotrophy and carbon storage potential [PhD thesis]. Stellenbosch University.

Nyaga, J.M., Cramer, M.D., Neff, J.C., 2013. Atmospheric nutrient deposition to the west coast of South Africa. *Atmos. Environ.* 81, 625–632. https://doi.org/10.1016/j.atmosenv.2013.09.021.

Palmieri, F., Estoppey, A., House, G. L., Lohberger, A., Bindschedler, S., Chain, P. S. G., & Junier, P. (2019). *Oxalic acid, a molecule at the crossroads of bacterial-fungal interactions* (pp. 49–77). https://doi.org/10.1016/bs.aambs.2018.10.001.

Parzych, K.R., Klionsky, D.J., 2014. An overview of autophagy: morphology, mechanism, and regulation. *Antioxid. Redox Signal.* 20 (3), 460–473. https://doi.org/10.1089/ars.2013.5371.

Pons, S., Bindschedler, S., Sebag, D., Junier, P., Verrecchia, E., Cailleau, G., 2018. Biocontrolled soil nutrient distribution under the influence of an oxalogenic-oxalotrophic ecosystem. *Plant and Soil* 425 (1–2), 145–160. https://doi.org/10.1007/s11104-018-3573-1.

Rowley, M.C., Estrada-Medina, H., Tzec-Gamboa, M., Rozin, A., Cailleau, G., Verrecchia, E.P., Green, I., 2017. Moving carbon between spheres, the potential oxalate-carbonate pathway of *Brosimum alicastrum* Sw.; Moraceae. Plant and Soil 412 (1–2), 465–479. https://doi.org/10.1007/s11104-016-3135-3.

RStudio Team. (2019). *RStudio: Integrated Development for R. RStudio*. PBC. http://www.rstudio.com/.

Sakala, B. (2023). *Carbon characteristics and the effect of terrain and cultivation on topsoil carbon and salts of the West Coast heuweltjies* [MSc thesis]. Stellenbosch University.

Seddon, N., Chausson, A., Berry, P., Girardin, C.A.J., Smith, A., Turner, B., 2020. Understanding the value and limits of nature-based solutions to climate change and other global challenges. *Philos. Trans. R. Soc., B* 375 (1794), 20190120. https://doi.org/10.1098/rstb.2019.0120.

Seyedsayamdost, M.R., 2019. Toward a global picture of bacterial secondary metabolism. *J. Ind. Microbiol. Biotechnol.* 46 (3–4), 301–311. https://doi.org/10.1007/s10295-019-02136-y.

Smart, K.E., Breecker, D.O., Blackwood, C.B., Gallagher, T.M., 2025. A new approach to continuous monitoring of carbon use efficiency and biosynthesis in soil microbes from measurement of CO_2 and O_2. *Biogeosciences* 22 (1), 87–101. https://doi.org/10.5194/bg-22-87-2025.

Swartland Area Information. (n.d.). Retrieved October 30, 2023, from https://www.agrisell.co.za/area-profiles/swartland/#:~:text=The%20climate%20here%20is%20mild,the%20K%C3%B6ppen%2DGeiger%20climate%20classification.

Syed, S., Buddolla, V., Lian, B., 2020. Oxalate carbonate pathway—conversion and fixation of soil carbon—a potential scenario for sustainability. *Front. Plant Sci.* 11 (December), 1–7. https://doi.org/10.3389/fpls.2020.591297.

Taylor, L.L., Quirk, J., Thorley, R.M.S., Kharecha, P.A., Hansen, J., Ridgwell, A., Lomas, M.R., Banwart, S.A., Beerling, D.J., 2016. Enhanced weathering strategies for stabilizing climate and averting ocean acidification. *Nat. Clim. Chang.* 6 (4), 402–406. https://doi.org/10.1038/nclimate2882.

Tooulakou, G., Giannopoulos, A., Nikolopoulos, D., Bresta, P., Dotsika, E., Orkoula, M.G., Kontoyannis, C.G., Fasseas, C., Liakopoulos, G., Klapa, M.I., Karabourniotis, G., 2016. Alarm photosynthesis: calcium oxalate crystals as an internal CO_2 source in plants. Plant Physiol. 171 (4), 2577–2585. https://doi.org/10.1104/pp.16.00111.

Uren, N.C., 2018. Calcium oxalate in soils, its origins and fate - a review. *Soil Res.* 56, 443–450.

van Gend, J., Francis, M.L., Watson, A.P., Palcsu, L., Horváth, A., Macey, P.H., le Roux, P., Clarke, C.E., Miller, J.A., 2021. Saline groundwater in the Buffels River catchment, Namaqualand, South Africa: A new look at an old problem. *Sci. Total Environ.* 762, 2020–2021. https://doi.org/10.1016/j.scitotenv.2020.143140.

Vázquez-Vuelvas, O.F., Cervantes-Chávez, J.A., Delgado-Virgen, F.J., Valdez-Velázquez, L.L., Osuna-Cisneros, R.J., 2021. Fungal bioprocessing of lignocellulosic materials for biorefinery. In: *Recent Advancement in Microbial Biotechnology*. Elsevier, pp. 171–208. https://doi.org/10.1016/B978-0-12-822098-6.00009-4.

Vermonti, N., 2022. *Structural and functional attributes of heuweltjies in the fynbos and succulent karoo biomes: the interaction of termites, vegetation and geochemistry* [MSc thesis]. Stellenbosch University.

Vermonti, N., Clarke, C.E., Crous, C.J., Miller, J.A., Nel, T., Francis, M.L., 2025. Termites as vectors for the lateral movement of elements in the landscape: Their influence on nutrient cycling and landscape heterogeneity. *Appl. Soil Ecol.* 206, 105898. https://doi.org/10.1016/j.apsoil.2025.105898.

Verrecchia, E.P., Braissant, O., Cailleau, G., 2006. The oxalate-carbonate pathway in soil carbon storage: The role of fungi and oxalotrophic bacteria. *Fungi in Biogeochemical Cycles* 24 (January), 289–310. https://doi.org/10.1017/CBO9780511550522.013.

Wang, Y., Konstantinou, C., Tang, S., Chen, H., 2023. Applications of microbial-induced carbonate precipitation: a state-of-the-art review. *Biogeotechnics* 1 (1), 100008. https://doi.org/10.1016/j.bgtech.2023.100008.